Georgia Institute of Technology
School of Electrical and Computer Engineering

Ohmic Contacts for Wide Bandgap Devices

By

Zen Mehra
Candidate for Bachelor of Science in Electrical Engineering

Undergraduate Honors Thesis
Presented to the Academic Faculty in Partial Fulfillment of Institute Requirements
for the Undergraduate Research Option

Zen Mehra
Undergraduate Student

Dr. Shyh-Chiang Shen
Faculty Advisor
Assistant Professor, School of Electrical & Computer Engineering

---

Dr. Russell Dupuis
Thesis Review Committee
Steve W. Chaddick Endowed Chair in Electro-Optics
Professor, School of Electrical & Computer Engineering

Dr. Douglas B. Williams
Associate Chair for Undergraduate Affairs
School of Electrical & Computer Engineering

Abstract

Bipolar devices based on GaN and SiC have gained tremendous popularity as an alternative to Si based devices, primarily due to the ability to sustain high temperature and high voltage operations that can be attributed to their high breakdown field and saturation velocity. Any bipolar device based on wide bandgap technology requires high performing ohmic contacts that have low specific contact resistivity and exhibit linear I-V behavior, as opposed to Schottky characteristics. A range of high work function metals like Ni, Au, Pd, Pt, Al can be used to realize these contacts. Further, annealing under specific conditions is required to ensure extremely high doping in the near surface layer. In this research, the Ni/Au stack for p-type contacts, and the Ti/Al/Ti/Au layer for n-type contacts have been specifically investigated over a range of annealing time periods and temperatures. Control wafers with GaN:Mg (p-type) or GaN:Si and GaN/AlGaN (n-type) formed the basis of this study. The Transmission Line Model (TLM) technique was used to conduct measurements, and obtain the specific contact resistance. Specific contact resistances as low as $9.44*10^{-3}$ Ω-cm^2 for n-type, and $5.73*10^{-3}$ Ω-cm^2 for p-type were achieved. These shall form the basis for ultimate fabrication of an InGaN/GaN HBT with a high current gain, breakdown voltage (V_{BR}) and current density (J). The quality of resulting contact is seen to depend on the initial doping/bulk resistance, determination of a unique time-temperature window, and careful process control. A further investigation is conducted into non-linear behavior exhibited by p-type contacts for low separation.

Table of Contents

1. Introduction and Background Study

1.1 Introduction

Wide bandgap materials like GaN have gained significant importance and recognition in the recent past, for their specific material properties that make them an attractive replacement to silicon for optoelectronic device applications. In particular, the high electron saturation velocity, high thermal conductivity, and wide temperature operation range capability allows GaN based devices to sustain high temperature operations up to 300C (the best Si based devices cannot operate at temperatures >100C). Heterojuction Bipolar Transistors (HBT) are transistors where the emitter/collector is designed to have a larger bandgap than the base. The added potential barrier prevents the injection of holes (in an n-p-n device) into the base, and enables it to overcome the limitations on gain and associated tradeoffs inherent to a traditional Bipolar Junction Transistor (BJT).

For the realization of any wide bandgap bipolar device, it is necessary to first fabricate high quality ohmic contacts that enable the device to be placed in a physical circuit application, and to ensure reliable and accurate device performance. The work done towards completing this thesis focuses on the study of optimized ohmic contacts for both ‘n’ and ‘p’ on GaN.

1.2 Background

1.2.1 Significance of Ohmic Contacts

An ohmic contact refers to the junction between a metal and semiconductor that allows carriers (electrons or holes) to flow into or out of the semiconductor in a process that is linear, i.e., the current is proportional to the voltage. It is a vital part of a solid state device, as any current passing through the device does so through the ohmic contact [1].

The ideal ohmic contact should thus have little or no effect on device performance, and must be capable of delivering the required current with negligible voltage drop between the metal and semiconductor. It must have an intrinsic contact resistance that is as small as possible in comparison to the bulk or spreading resistance of the semiconductor. A high contact resistance could cause power dissipation through joule heating in analog circuits. The RC time constant associated with such a resistance can also limit the frequency response of such devices. The current-voltage (I-V) curve of the contact should ideally be linear and symmetric, as theoretically expected. Processing parameters used during its fabrication can have a limiting impact on the remaining device synthesis. Thus, it is very important to develop a good ohmic contact prior to the realization of any device [2], [3].

The theoretical basis for ohmic contacts lies in understanding potential barriers and current mechanisms through a metal-semiconductor junction. When two materials are placed in contact, electrons flow from one with the lower work function until the two Fermi levels equate. A built-in field and contact potential is set up at the interface, caused by ‘bending’ of the valence and conduction bands. In classical physics, the only way for

an electron to surmount this barrier would be to acquire enough thermal energy to overcome the potential, known as thermionic emission. Quantum mechanically, however, an electron could 'tunnel' through the barrier if it is sufficiently narrow and the doping on either side large enough. Thermionic emission induces Schottky behavior in a contact (exponential I-V characteristics) and should be avoided, and the probability of tunneling increased as much as possible. For a p-type semiconductor, this means that the work function of the metal must be close to or larger than the sum of the electron affinity and the bandgap energy of the semiconductor. For an n-type semiconductor, this means that the work function of the metal must be close to or smaller than the electron affinity of the semiconductor. Figure 1 shows the energy band diagrams for an n-type semiconductor in contact with a metal [1], [4].

The realization of these contacts requires a thin, very highly doped layer at the interface. The technique for GaN devices is to use a metal with an appropriate bandgap, such as Ti, Al, Au, Ni or a combination, on a highly doped wafer. Annealing the structure at a high temperature in an air/nitrogen ambient causes the dopants/metal to alloy with the semiconductor, forming a thin high-doped region as desired for a tunnel contact [2], [5].

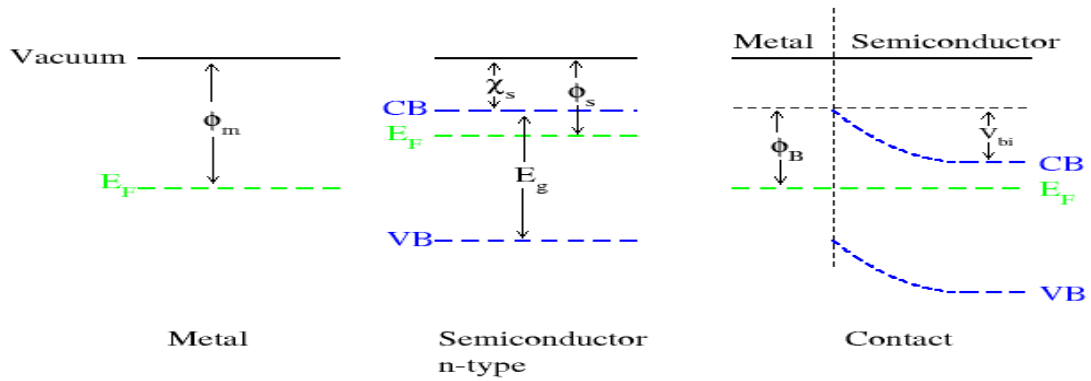

Figure 1. Energy band diagrams for a metal-semiconductor contact [4].

1.2.2 p-Type Ohmic Contacts

For light emitting diodes, laser diodes, and other optoelectronic applications, the fabrication of p-type ohmic contacts has been a rather challenging task due to the low activation efficiency of Mg dopants and the tendency of the GaN surface to preferentially lose N during processing. Single layer, bilayer, and multilayer metallization schemes based on high work function metals (Ni, Pt, Au, Pd) and inter-metallic compounds have been the materials of choice for contact formation [6].

The high work function and reactivity of Pd make it suitable for ohmic contact formation at low processing temperatures. Pd/Au contacts have been found to exhibit lower contact resistances, possibly owing to Pd acting as an acceptor in GaN, causing the near surface region to be highly doped. The Ni/Pd/Au stack has been used to obtain low resistance contacts on highly doped p-GaN (N_A=2.8*10^{18} cm^{-3}) [7]. Pd placed directly in contact with moderately doped p-GaN (N_A=2*10^{17} cm^{-3}) has shown linear behavior with specific contact resistivity as low as 4.3*10^{-4} Ω-cm^2 [8]. An investigation into the Pd/Ni/Au metallization annealed at 500C for 1min in flowing N_2 ambient showed a contact resistivity of 2.4*10^{-5} Ω-cm^2 [6].

Au/Ni based contacts, when annealed in oxygen ambient, are capable of producing specific contact resistivity in the range of 10^{-2} to 10^{-6} Ω-cm^2. Research shows that this is due to the increase of hole concentration in the near surface region, caused by the removal of hydrogen atoms in the presence of oxygen [9]. Qiao, et al. in their work on (Au~200 Å/Ni~200 Å) structures showed that it is essential to form a structure of Au and Ni in the proper deposition sequence before annealing it in oxygen containing ambient. The presence of oxygen was studied to cause the increase of p-GaN conductivity, and Ni

to reduce the surface contamination of the GaN sample before or during layer reversal [10]. In the case of optoelectronic devices, transparency, or the amount of light passed through a layer structure, as well as its uniformity, can be key issues. A Ni/Au setup with thicknesses of 2nm, and 6nm, respectively, can show a transmittance of up to 88% @ 470nm, when annealed at 500C for 5min. This can be achieved without using traditional Indium Tin Oxide (ITO) films. The light transmission is seen to increase with alloying temperature due to the gradual decrease in Ni thickness as a consequence of Ni diffusion, and its reaction with GaN at the metal/semiconductor interface [11].

The role of heat treatment in altering ohmic characteristics has been thoroughly considered. An optimum time and temperature combination has to be determined, which can provide the lowest contact resistance. As an example, the contact resistance of a Ni/Au metallization reduces from $1.2*10^{-2}$ Ω-cm^2 after treatment at 300C to $4*10^{-6}$ Ω-cm^2 after treatment at 500C. It increases, however, to $3.2*10^{-3}$ Ω-cm^2 after treatment at 600C. The reduced resistance is caused by epitaxial construction of the NiO film and Au islands on a p-type GaN epitaxial layer. The decrease at higher temperatures is attributed to the interfacial reaction that releases more N_2, enlarging the lattice voids. These voids separate the crystalline NiO from p-type GaN, reducing the contacting area and increasing resistance [12].

1.2.3 n-Type Ohmic Contacts

Owing to very wide band gaps of nitrides, n-type contacts are vastly different from those of GaAs, InP, and Si. As in p-type contacts, various combinations of layer structures involving Ti/Al/Au/Ni have been used over a range of annealing temperatures, times, and varying surface treatment methodologies [13].

Fan, et al. used a Ti/Al/Ni/Au (150Å/2200 Å/400 Å/500 Å) structure on n-GaN with annealing at 900C for 30s, resulting in a specific contact resistivity of $\rho_s = 8.9*10^{-8}$ Ω-cm^2. However, the metallization in this case was preceded by a reactive ion etch (RIE) process using Cl_2 and BCl_3. The damage caused by the RIE is said to significantly lower the resistance. This is because unless the semiconductor itself is altered with damage such as increased electron concentration due to nitrogen vacancy formation, it is difficult to form an ohmic contact to GaN given its wide energy band gap of 3.42 eV, generally due to the fact that a metal does not exist with a low enough work function to yield a low barrier to current transport [14].

A high transparency Ni/Au bi-layer contact has been achieved, using a 500 Å/250 Å layer metallization, resulting in $\rho_s = 6.9*10^{-6}$ Ω-cm^2. More importantly, the high optical transmission achieved (in the range of 400–700 nm, peaking at 88% when $\lambda = 470$ nm) through this contact after annealing suggests that it is indeed very useful for electro-optic device applications. The presence of only (111) Au and (111) Ni peaks in the x-ray diffraction patterns of these samples indicates that both metals participate to form epitaxial or highly textured layers on the basal GaN plane. When the contact layer is annealed, Au and Ni react with GaN creating interfacial phases. The Ni_3Ga and Ni_2Ga_3

intermetallic phases possess a low work function, lowering the contact resistance of the system [14].

An interesting experiment conducted by Guo, et al. showed that a heavily doped contact layer is sufficient for lowering the contact resistance, even without any sort of annealing. 15 nm Ti deposited directly on GaN, followed by a 150 nm Ag top layer results in a specific contact resistivity of $6.5*10^{-5}$ Ω-cm^2 without thermal annealing at a doping concentration of $1.7*10^{19}$ cm^{-3}. The barrier height of Ti under these conditions is calculated to be 0.067 eV, which allows the tunneling current process to dominate. In this structure, Ag helps counter the high resistivity of Ti, as a nonzero metal overlay sheet resistance can significantly alter the effective contact resistance value. A thin Ti and a thick Ag top layer helps achieve this goal [15].

Apart from experimenting with layer structures, good results can often be obtained by changing the bulk wafer composition. Utilizing a thin n-type $Al_xGa_{1-x}N$ layer on top of n-type GaN, the metal–semiconductor contact resistance can be decreased drastically compared to bulk n-type GaN. Specific contact resistances as low as 10^{-8} Ω-cm^2 can be achieved by using an alloyed Ti/Al/Ni/Au metallization scheme on this modified layer. This phenomenon can be explained by the occurrence of spontaneous polarization fields within the crystal. Because of its wurtzite crystal structure, the III-nitride material system can support spontaneous polarization fields. Significant fields are also induced due to piezoelectric effects, both of which bend the conduction and valence bands resulting in the formation of a two-dimensional electron gas. In the case of a thin $Al_xGa_{1-x}N$ layer grown on top of n-type GaN, the polarization fields can be utilized to

decrease the contact resistance by increasing the tunneling probability through the top layer [16].

The effect of chemical surface treatment on n-type contacts, $(NH_4)_2S_x$ in particular, has shown to reduce readings to $5.0*10^{-5}$ Ω-cm^2 for the Ti/Al non-alloyed ohmic contact. By using $(NH4)_2S_x$, not only are the native oxide (Ga-O bonds) removed, but Ga–S bonds formed and nitrogen-related vacancies occupied. This causes the deposited Ti to be in intimate contact with the cleaned GaN surface, easily forming TiN and thus improving device performance [17].

1.2.4 TLM Measurement Technique

The Transmission Line Measurement (TLM) technique was used to determine both the contact and sheet resistance of each ohmic contact. In this technique, two probes are applied to a pair of contacts, and the resistance between them measured by applying a voltage across the contacts and measuring the resulting current. The current flows from the first probe, across the ohmic contact, and back into the second probe. A semiconductor parameter analyzer or ammeter can be used to measure this current over known stepped voltages, and Ohm's law (V=IR) used to determine the resistance. The resistance measured so far, however, is the sum of the contact resistances of both the contacts, and the sheet resistance of the semiconductor in between the contacts.

On making a complete set of measurements (one for each contact spacing), a plot of resistance versus contact separation can be obtained. Such a plot should ideally be linear, with the y-intercept being the contact resistance (R_1), and its slope the semiconductor resistance (R_2). Equations 1 and 2 outline the extraction of the specific contact resistance and bulk resistance of the wafer from these quantities [4].

$$R_1 = \frac{\rho_c}{Wl} \qquad (1)$$

$$R_2 = R_s \frac{l}{W} \qquad (2)$$

where R_1 - measured contact resistance
R_2 - measured semiconductor resistance
ρ_c - specific contact resistance
R_s - bulk resistance
W – width of TLM spacing
l - length of TLM spacing

The regression coefficient obtained through a linear curve-fit is calculated, in general, by

$$r = \frac{n\sum(xy) - \sum x \sum y}{\sqrt{n\sum(x^2) - \left(\sum x\right)^2 n\sum(y^2) - \left(\sum y\right)^2}} \qquad (3)$$

where r - regression coefficient
n – number of data points
x – independent variable (voltage)
y – dependent variable (current)

Figure 2 shows sample I-V data obtained for one particular contact spacing. Figure 3 shows the resistance versus contact separation plot obtained after a linear regression of five such data points is performed.

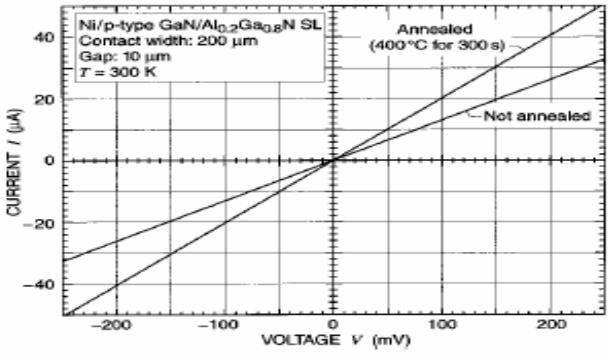

Figure 2. I-V data obtained using TLM technique [18]

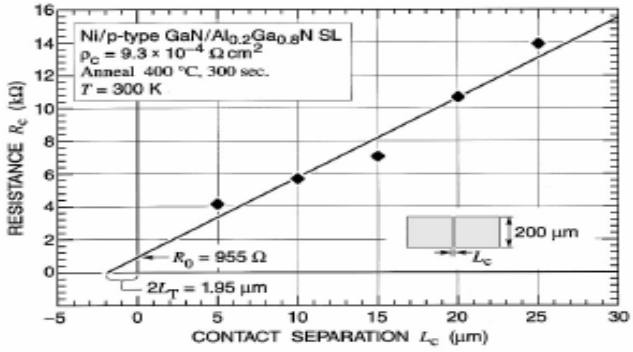

Figure 3. Resistance data obtained after regression [18].

2. Experiment Design and Process Layout

2.1 Research Objectives

The investigation into ohmic contacts on GaN devices was divided into two parts:

1. a study of different layer structures and annealing temperatures on control wafers that had various doping content, in order to obtain the best possible ohmic contact;
2. a detailed case study on one particular AlGaN/GaN wafer that focused on establishing the ideal time-temperature window for optimum linearity and contact resistance.

2.2 Fabrication Process

Preliminary Wafer Data

Five different wafers were used during the course of this investigation. Table 1 outlines the preliminary wafer data for the contact wafers under investigation.

Wafer Number	Type	Composition	Mobility (cm^2/Vs)	Doping (cm^{-3})	Bulk Resistance (Ω-cm)
2-0506-5	p	GaN:Mg	2.13	$7.87*10^{17}$	3.72
2-0507-5	p	GaN:Mg	2.42	$7.18*10^{17}$	3.59
2-1032-2	n	AlGaN	*	*	*
1-0906-2	n	GaN:Si	*	*	*
1-0722-5	n	GaN/AlGaN	55	$2*10^{18}$	0.05

Table 1. Preliminary wafer data.

Cleaning and Initial Treatment

Each wafer was cleaned using a sequence of three solvents to remove organic, inorganic, and physical impurities such as dust or excessive moisture. Acetone, methanol,

isopropanol were used in that order. The wafers were then heated for 5min at 60C immersed in each solution and dried using pressurized nitrogen.

Photolithography

Before photolithography, every sample was pre-baked at 110C for 5min to remove excessive moisture or chemical residue. Hexa Methyl Di Silazane (HMDS), used as a primer, was coated on the wafer surface by spinning it at 500 rpm for 30s in the CEE-100 AUTO DISP wafer spinner. The LOR10B was used as a positive photoresist, and applied using the same recipe in the spinner. An edge cleaning process followed, using the 1165 stripper that helped remove excess photoresist from wafer edges, thereby ensuring better contact during exposure. An intermediate bake at 170C for 5min was carried out before applying the S1813 photoresist as the third and final layer. A post-bake at 110C for 1min and another edge cleaning process helped prepare the wafer for exposure.

During exposure, the mask was first aligned correctly in order to maximize the number of TLM pattern sequences that would be imprinted on the surface. I-line ultraviolet light (λ=365nm) under a 45s exposure time projected the mask pattern under the Karl Suss MJB-3 exposure system.

The MF-319 developer was to develop the pattern for 35s. This step was found to be the most crucial in the processing sequence, as even a minor alteration in the development time had drastic consequences on the quality of the resulting pattern.

Surface Treatment

Prior to evaporation, chemical surface treatment was performed using a Buffered Oxide Etch (BOE) 6:1 solution diluted with 50% water, through a rinse period of 15s.

This step has shown to remarkably alter the characteristics post-metallization, and has been recorded in literature as crucial to lowering contact resistance.

Metallization

Metal layers were deposited onto the wafer by using a CHA Process Development Solution metallization system. Kurt J. Lesker solid sources were used as the metal supply. Table 2 shows the metallization scheme used for each wafer.

Wafer	Metal	Thickness (Å)
2-0506-5	Ni/Au	200/200
2-0507-5	Ni/Au	200/200
2-1032-2	Ti/Al/Ti/Au	300/500/300/500
1-0906-2	Ti/Al/Ti/Au	300/500/300/500
1-0722-5	Ti/Al/Ti/Au	300/500/300/500

Table 2. Metallization scheme used for each wafer.

Annealing

Annealing was performed using an AnnealSys AS-One Rapid Thermal Annealing (RTA) system, and was carried out in an air ambient for all p-type samples, and nitrogen ambient for all n-type samples.

3. Results

For the first part of this study, both I-V and regression data was obtained for each sample, from which the contact resistance was determined from TLM theory. The specific contact resistance (R_c) was obtained by multiplying the contact resistance by area of the TLM pattern. The data points obtained through regression were curve fitted to a straight line. The regression or "goodness" coefficient (R^2) computed through the least squares method indicates the relative closeness or fit of the data to a straight line, and is computed using the standard deviation from the mean of each reading, as outlined earlier.

Only those readings with $R^2 > 0.99$ have been shown in this section, and others discarded for lack of measurement accuracy. For the second part of this investigation (GaN/AlGaN wafer case study), only the final contact resistance for each time-temperature point is shown. Data points where the I-V curve was too non-linear to prevent an accurate contact resistance measurement were noted.

The principal sources of measurement error were as follows:

1. Probe Resistance – Each of the probe tips in the measurement station has a finite, non-zero resistance that was never accounted for. When tips were damaged or bent, they were replaced and the new tips often had a different resistance associated with them. Thus, the actual voltage across a spacing was lower than its theoretical value, due to a drop across the probe tips.
2. Pressure Variation – The pressure applied on a contact spacing from the tip is a crucial parameter in accuracy, and has to be closely controlled to ensure replication. Often, human error means that this pressure varies for each reading, which could contribute to a discrepancy in data.

A preliminary decision as to the nature of a contact can often be arrived at without extensive calculations. An exponential I-V curve indicates Schottky behavior, and the existence of thermionic current flow. As process parameters are refined, a good result will show an appreciable linearity, which indicates the realization of a good ohmic contact. In the case of p-type contacts in particular, it is often necessary to step up the input voltage to a higher degree than n-type (-20V to + 20V as compared to -2V to 2V), in order to observe sections that are sufficiently linear for a resistance estimate to be conducted.

3.1 Detailed Wafer Measurement Data

Wafer Number: 2-0506-5
Anneal Conditions: 550C for 7min
R_c: $3.68*10^{-2}$ Ω-cm^2 , R_s = 8.75 kΩ
Regression Coefficient: 0.9975

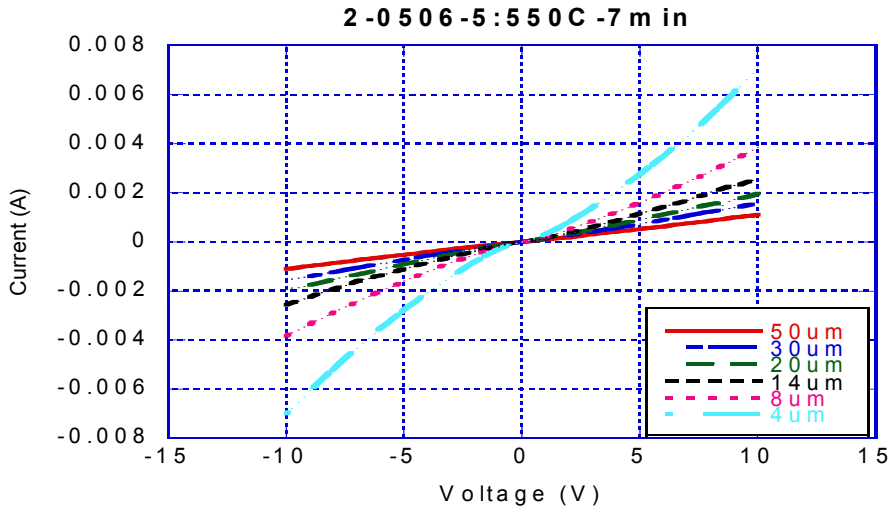

Figure 4. I-V data for 2-0506-5:550C-7min.

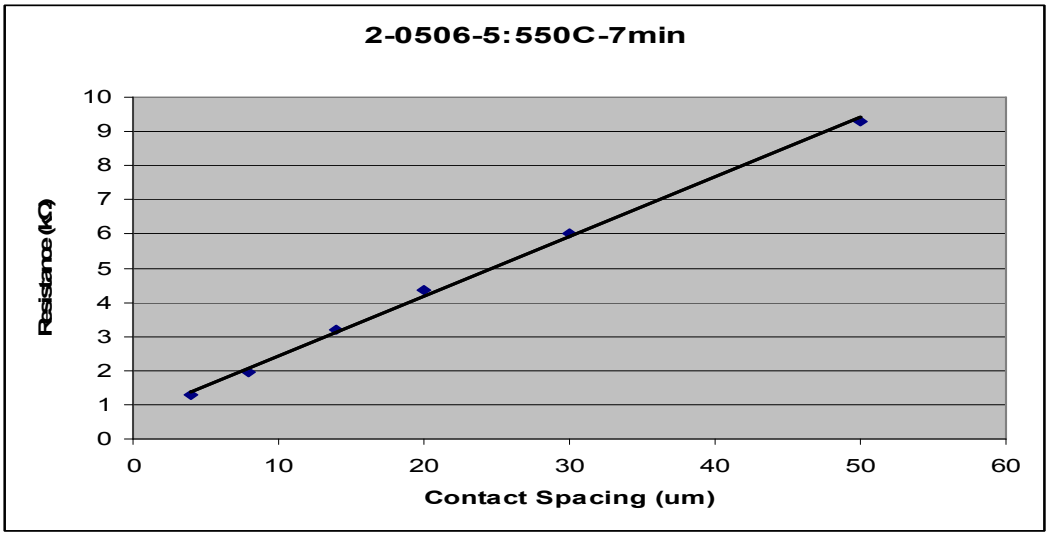

Figure 5. Regression data for 2-0506-5:550C-7min.

Wafer Number: 2-0506-5
Anneal Conditions: 600C for 30s
R_c: 4.43*10^{-2} Ω-cm^2, R_s = 7.93 kΩ
Regression Coefficient: 0.9984

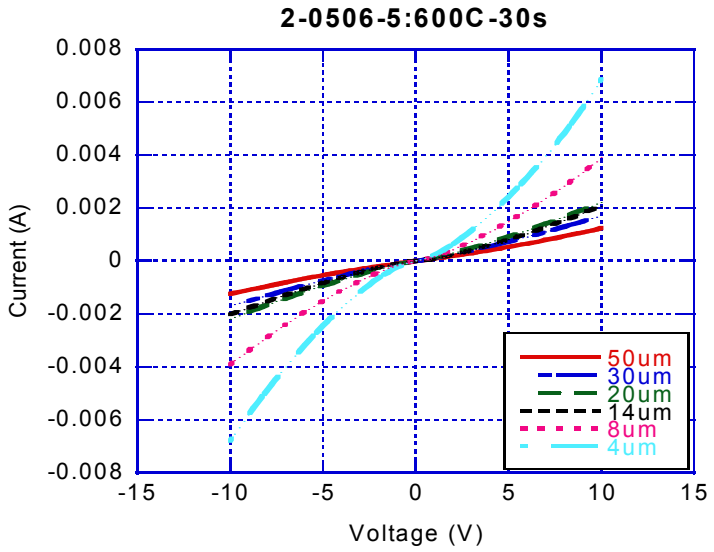

Figure 6. I-V data for 2-0506-5:600C-30s.

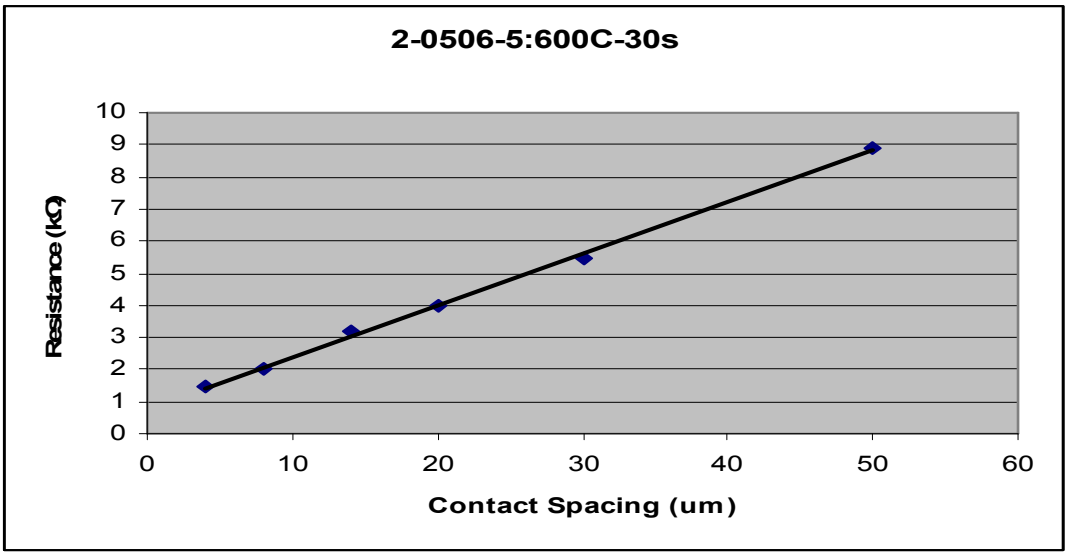

Figure 7. Regression data for 2-0506-5:600C-30s.

Wafer Number: 2-0507-5
Anneal Conditions: 550C for 50s
R_c: 5.73*10^{-3} Ω-cm^2, R_s = 6.68 kΩ
Regression Coefficient: 0.9970

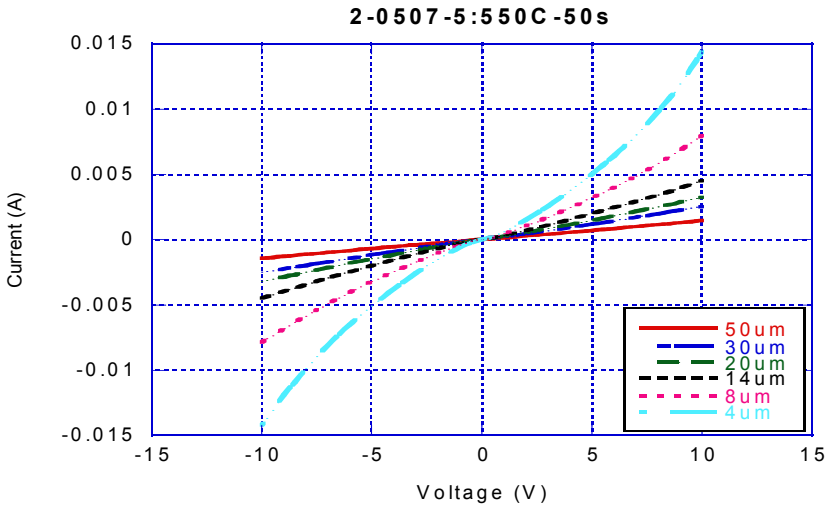

Figure 8. I-V data for 2-0507-5:550C-50s.

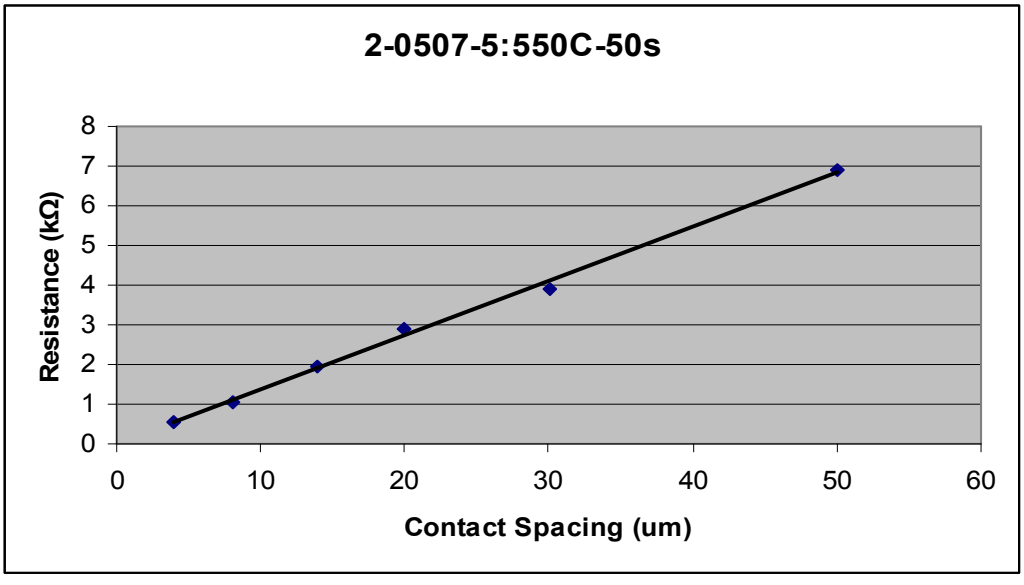

Figure 9. Regression data for 2-0507-5:550C-50s.

Wafer Number: 2-0507-5
Anneal Conditions: 600C for 1min
R_c: $1.85*10^{-2}$ Ω-cm^2, R_s = 5.37 kΩ
Regression Coefficient: 0.9938

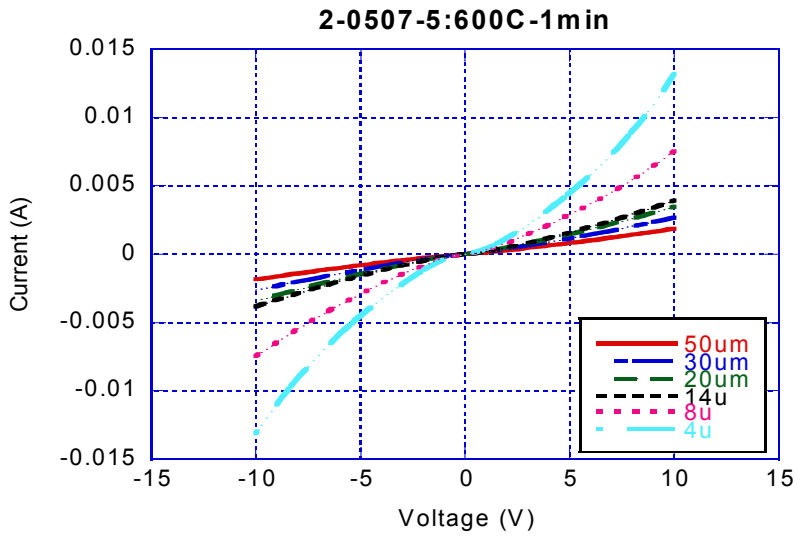

Figure 10. I-V data for 2-0507-5:600C-1min.

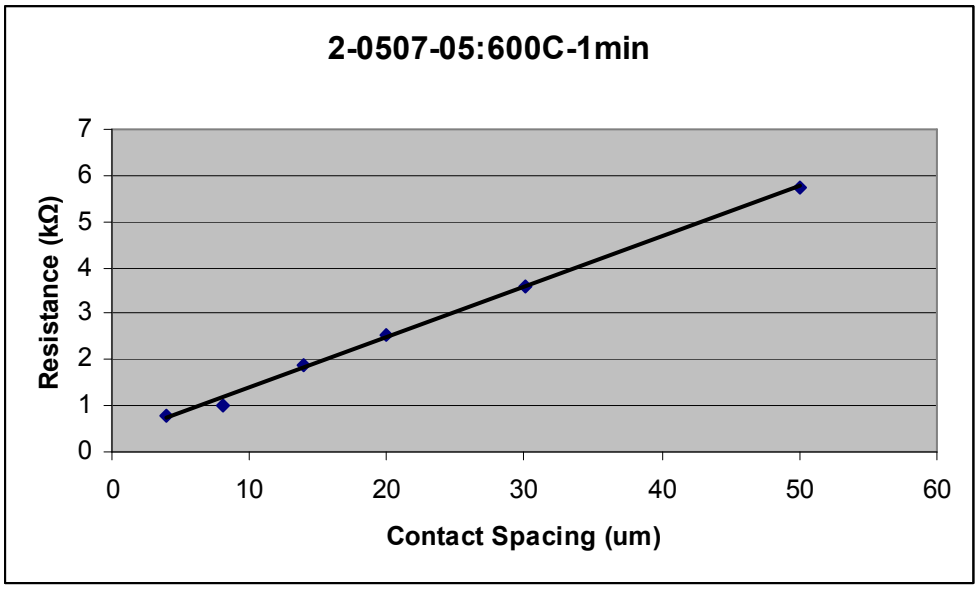

Figure 11. Regression data for 2-0507-5:600C-1min.

Wafer Number: 2-0506-5
Anneal Conditions: 600C for 1min
R_c: $3.11*10^{-2}$ Ω-cm^2, R_s = 8.06 kΩ
Regression Coefficient: 0.9983

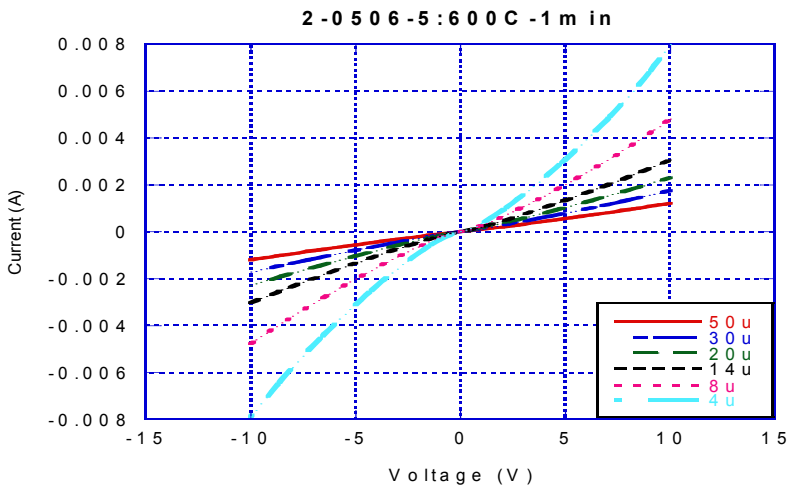

Figure 12. I-V data for 2-0506-5:600C-1min.

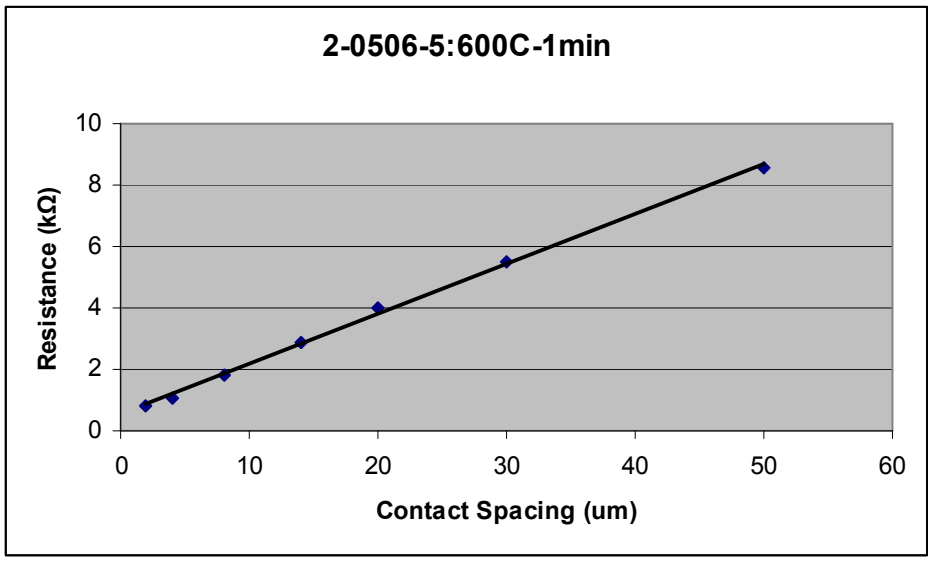

Figure 13. Regression data for 2-0506-5:600C-1min.

Wafer Number: 2-0506-5
Anneal Conditions: 550C for 2min
R_c: 2.77*10^{-2} Ω-cm^2, R_s = 7.81 kΩ
Regression Coefficient: 0.9963

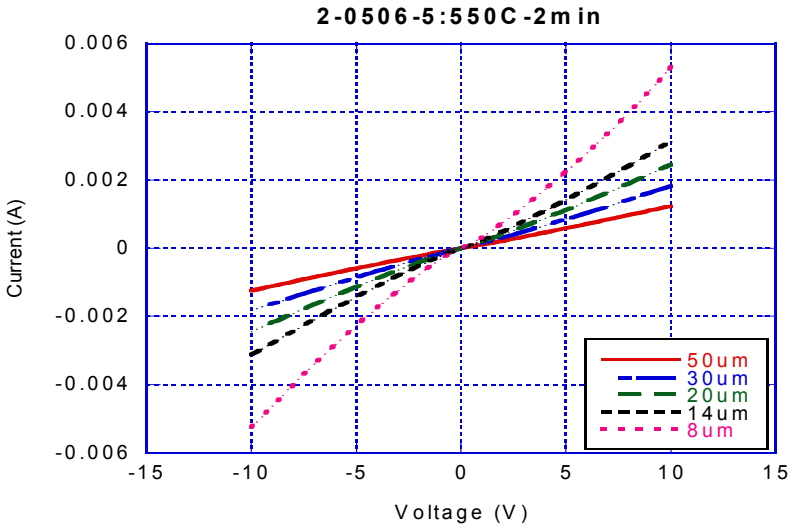

Figure 14. I-V data for 2-0506-5:550C-2min.

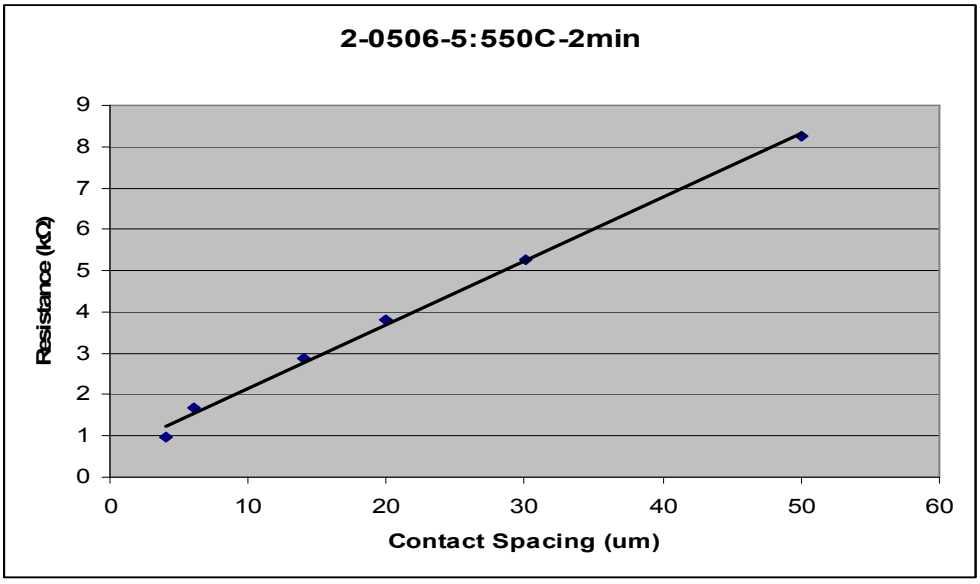

Figure 15. Regression data for 2-0506-5:550C-2min.

Wafer Number: 2-0506-5
Anneal Conditions: 550C for 1min
R_c: $4.16*10^{-2}$ Ω-cm^2, R_s = 7.92 kΩ
Regression Coefficient: 0.9902

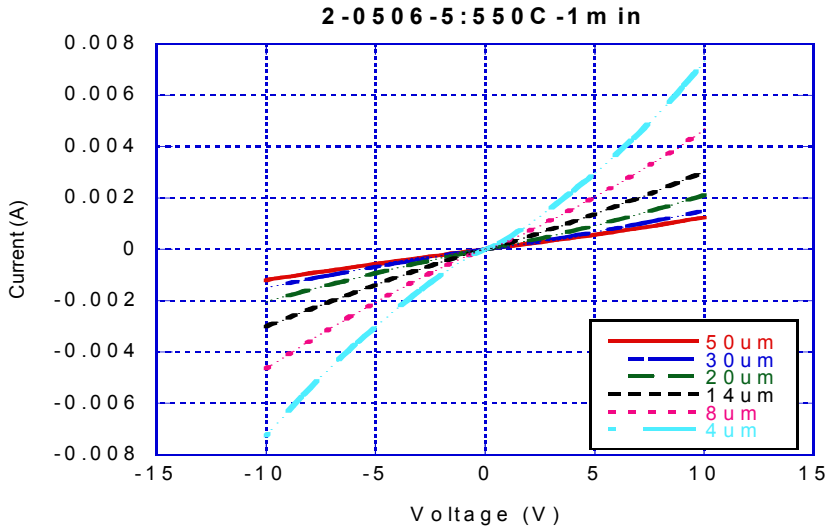

Figure 16. I-V data for 2-0506-5:550C-1min.

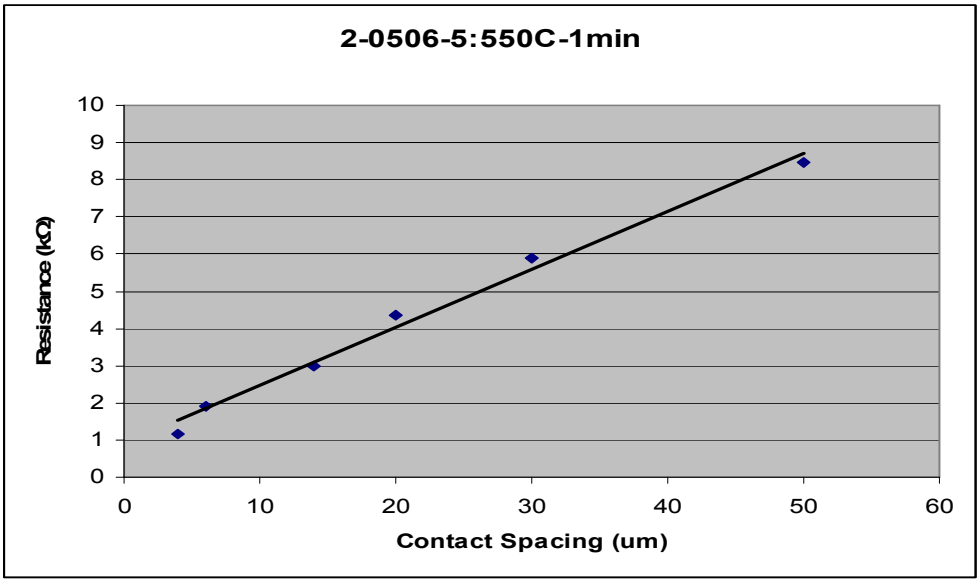

Figure 17. Regression data for 2-0506-5:550C-1min.

Wafer Number: 1-0906-2
Anneal Conditions: 750C for 1min
R_c: 2.72*10^{-3} Ω-cm^2, R_s = 82.3 Ω
Regression Coefficient: 0.9983

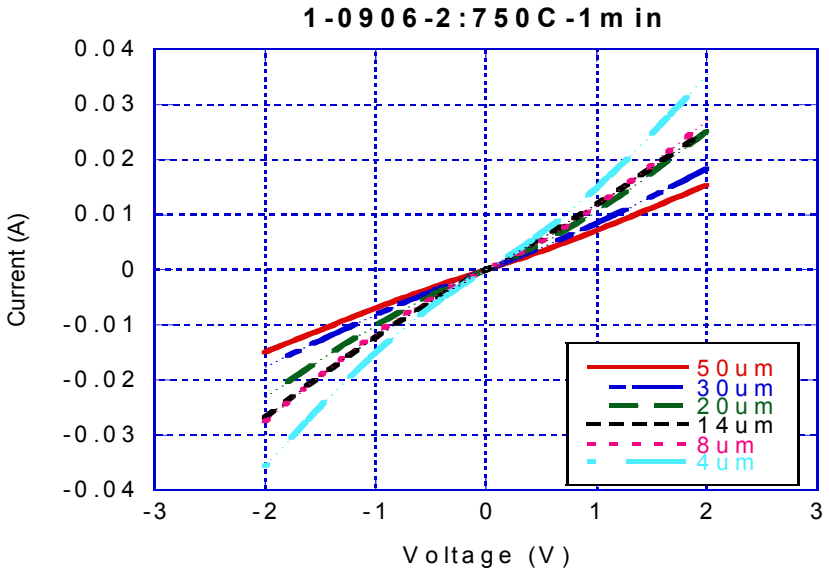

Figure 16. I-V data for 1-0906-2:750C-1min.

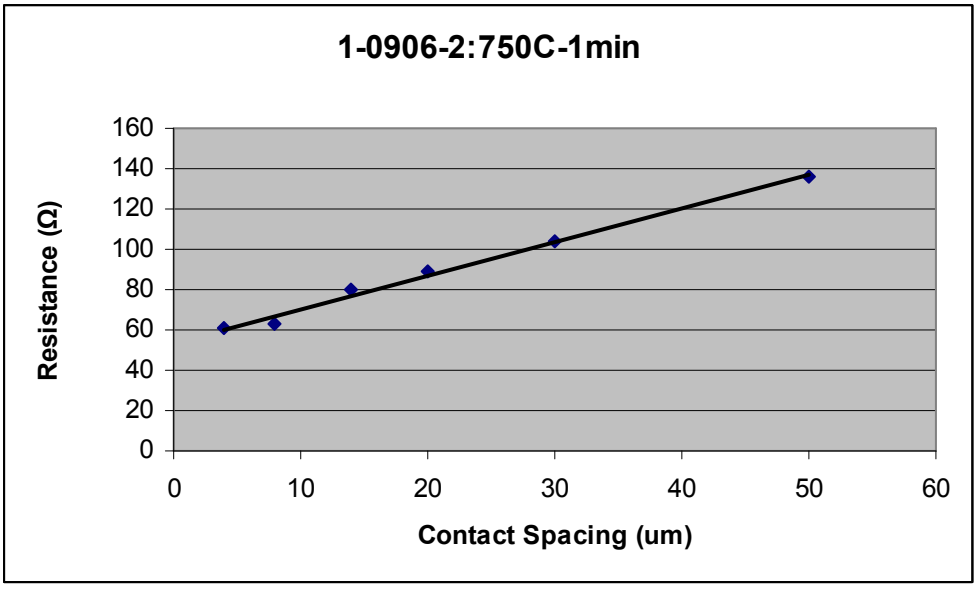

Figure 17. Regression data for 1-0906-2:750C-1min.

Wafer Number: 1-0722-5
Anneal Conditions: 850C for 30s
R_c: $9.44*10^{-3}$ Ω-cm^2, R_s = 1.05 kΩ
Regression Coefficient: 0.9901

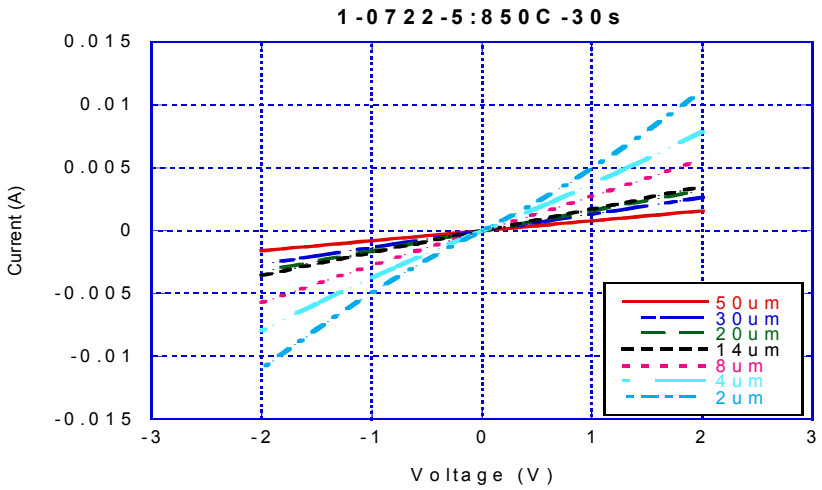

Figure 18. I-V data for 1-0722-5:850C-30s.

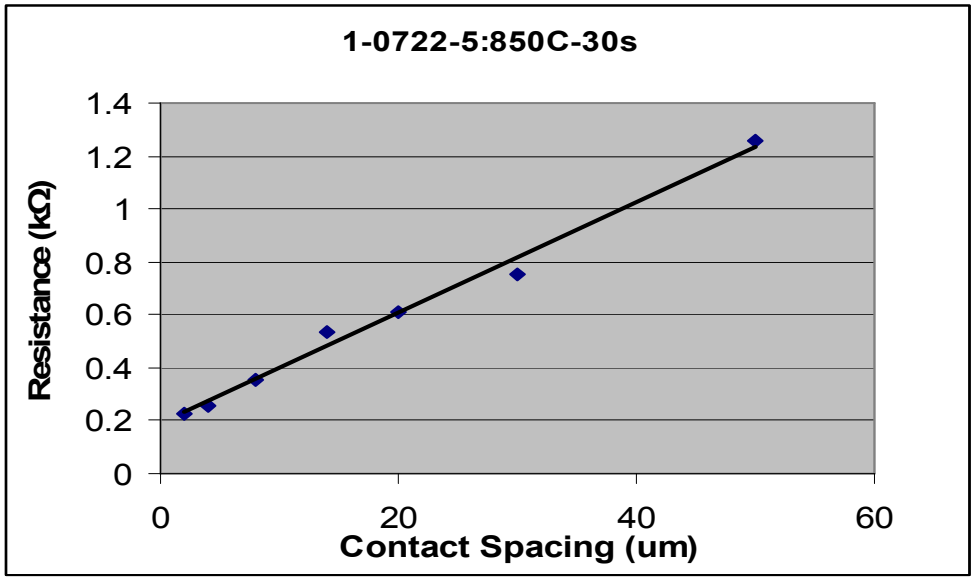

Figure 19. Regression data for 1-0722-5:850C-30s.

3.2 Non-Ohmic behavior in p-type GaN

In the preceding segment, data only up to the 4um contact spacing was shown for p-type contacts, and used to calculate the contact resistance. The I-V curve corresponding

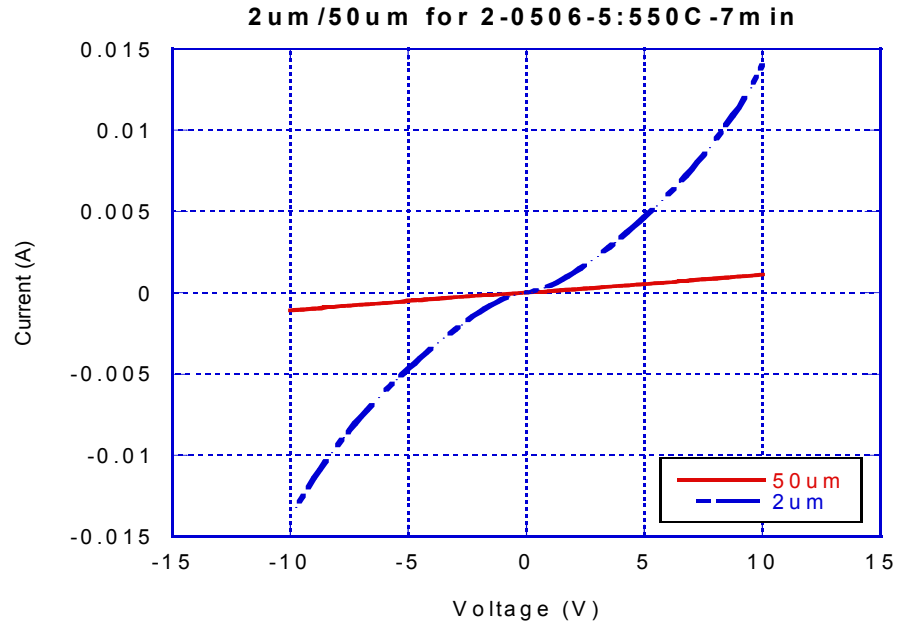

Figure 20. Isolated 2um/50um data for 2-0506-5 at 550C-7min.

to the 2um contact spacing was not displayed, and the corresponding data point not included in resistance calculations. This was due to the extensive non-linearity observed, from which it was impossible to accurately extrapolate any data. Figure 20 shows both 2um and 50um data from the 2-0506-5 wafer annealed at 550C for 7min. It amply illustrates the non-linear nature of the 2um curve in comparison with its 50um counterpart. At such a low contact spacing, the bulk resistance of the wafer is too low to prevent the Schottky effect from completely disappearing. Thermionic emission

continues to dominate as a means of electron transport, as opposed to quantum tunneling. Thus, an appreciably linear result is hard to achieve in this case given process limitations. Figure 21 shows a SPICE circuit used to simulate the above condition, where a Schottky diode model implemented by Fort-Hantgan is used to simulate the ohmic-Schottky combination that exists in a typical p-type contact [19]. The default SPICE diode model was tweaked to bring it in line with Ni/Au on GaN properties. In particular, the saturation current (I_s) and emission coefficient (N) were changed from their default values.

As shown in Figure 22, the simulation results match closely to the measured experimental data obtained.

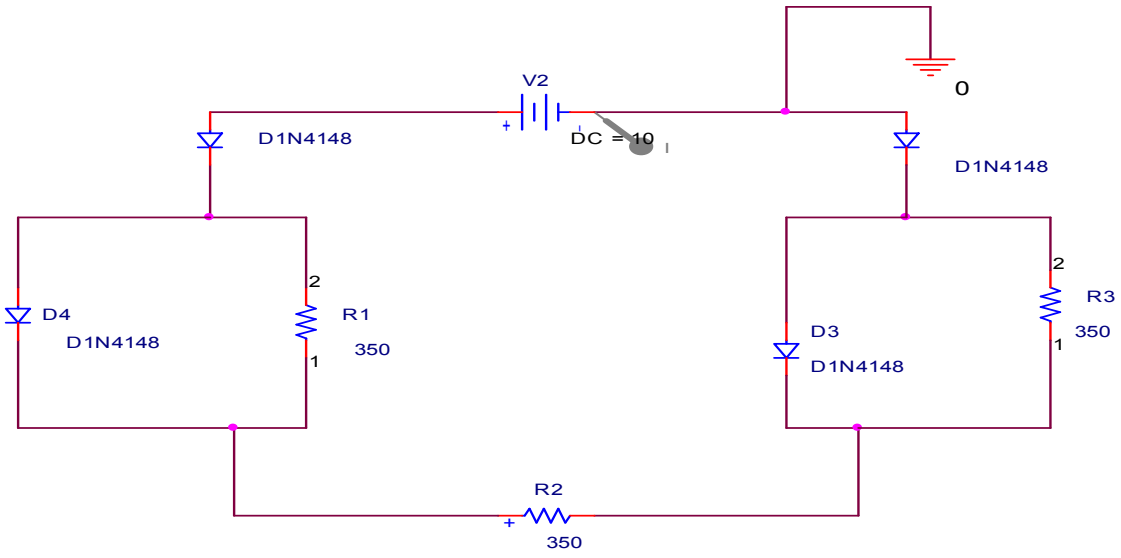

Figure 21. Circuit used to simulate Schottky-ohmic behavior.

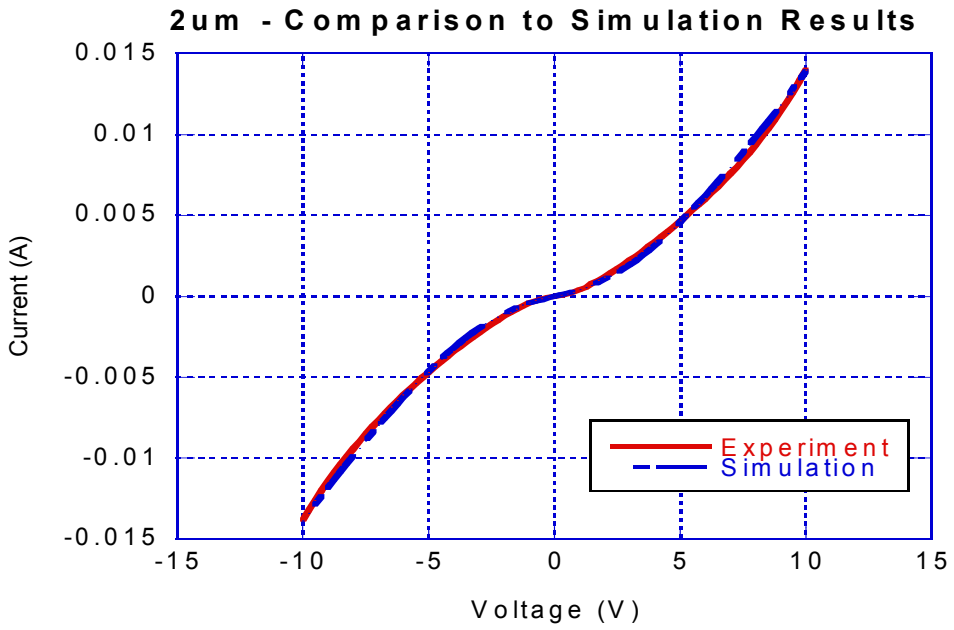

Figure 22. PSPICE simulation results for Schottky-ohmic behavior.

3.3 GaN/AlGaN Wafer Case Study

Figure 23 shows combined data from the single wafer case study conducted on the 1-0722-5 sample. Temperatures from 750C to 850C in steps of 50C were investigated. Annealing time periods from 30s to 90s in steps of 30s were used. Points for which the I-V graph was too non-linear for any acceptable measurement to be made were ignored, and an arbitrary high value assigned to them. While a number of local minima can be noticed over short regions, the graph converges to an absolute minima at (750C, 90s) which confirms the existence of a unique time-temperature window for which lowest contact resistance can be obtained. The effect of 'over-cooking' can be

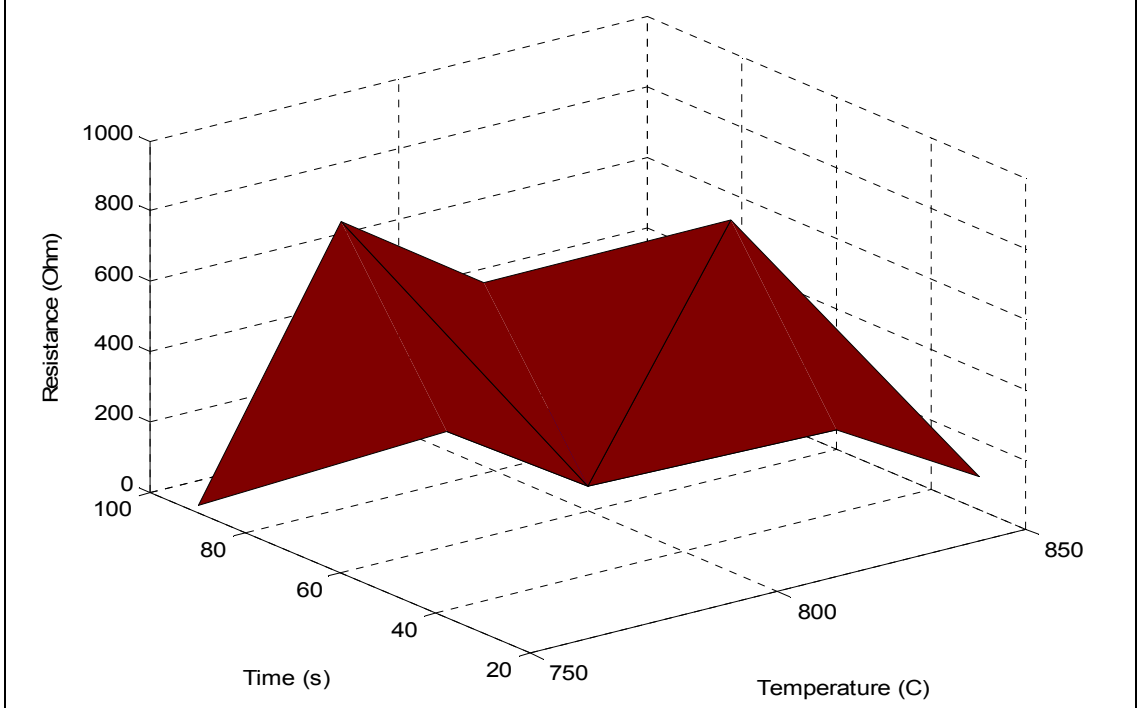

Figure 23. Resistance variation over time-temperature for GaN/AlGaN wafer.

starkly observed as almost every reading corresponding to 850C gives a resistance higher than that at lower temperatures. The impact of varying two variables simultaneously is also noted, as (800C, 90s) gives you a reading very close to (850C, 60s), which indicates a similarity in the total energy provided to the sample under these conditions.

4. Conclusions

Under similar metallization schemes and annealing conditions, it was easier to realize a good ohmic contact on a wafer that had a higher doping content and lower bulk resistance. In particular, almost every trial run done on the 2-0507-5 wafer showed better results than the exact same conditions used on the 2-0506-5, both in terms of linearity and

contact resistance. This could also be attributed to intangible factors like quality of the wafer or substrate or material growth conditions.

There exists a unique time-temperature window that allows for the lowest contact resistance. Any deviation in the form of 'under-heating' or 'over-cooking' leads to an increase in resistance. The extensive data shown for 2-0506-5 best illustrates this. Starting the trend at (550C, 1min) where a resistance of $4.16*10^{-2}$ Ω-cm^2 is recorded, the readings improve at (550C, 2min) where $2.77*10^{-2}$ Ω-cm^2 is the measured resistance. However, increasing this to (550C, 7min) degrades the results, increasing the resistance back to $3.68*10^{-2}$ Ω-cm^2. A more significant shift is seen with increasing temperature to (600C, 30s) whish shows $4.43*10^{-2}$ Ω-cm^2 and goes further down at (600C, 1min) to $3.11*10^{-2}$ Ω-cm^2. Since annealing equipment differs in every research environment, it is thus vital that each setup be calibrated and a vital process window established.

Specific conditions such as concentration of BOE solution, exposure time, and cleanliness of processing environment can produce vastly different results on the same wafer. During the test runs, different resistance values were often obtained on pieces of the same control wafer even when conditions were maintained as closely as possible. This is due to the fact that minor changes in moisture and humidity levels in the cleanroom, particulate matter on beakers, and pressure levels of incoming nitrogen could have made a difference. Hence the need for validation (same conditions on two different pieces) and consistency in experimental methods.

A vast difference in results was noted for n and p type contacts. It was significantly easier to achieve both linearity and a low resistance value for n-type contacts, and a peak reading of $2.72*10^{-3}$ Ω-cm^2. On the other hand, no measurement better than $5.73*10^{-3}$ Ω-

cm^2 could be obtained in the case of p-type ohmic contacts. Further, the 2um reading had to be dropped while conducting the regression analysis for p-type contacts, as data was too non-linear to enable a measurement. No such conditionality existed as far as n-type contacts This has been attributed to the low activation efficiency of Mg dopants and the tendency of the GaN surface to preferentially lose N during processing. In summary, while experimenting with Ni/Au/Ti/Al over the time-temperature range described above did yield good results, further investigation using Pt/Pd and a wider process range could potentially provide a better ohmic contact.

5. Future Work

The ohmic contact study that formed the background of this thesis provided vital data needed to realize contacts for almost any device fabricated in the future. In particular, the ultimate objective of the proposed research is to fabricate an InGaN/GaN HBT with a high current gain, breakdown voltage (V_{BR}) and current density (J), while ensuring reliable device operation at temperatures up to 300C.

6. Acknowledgements

I would like to thank Dr. Shyh-Chiang Shen for his continued support, understanding, and guidance for the past two years. It all began with a course in device physics back in junior year that made me want to further explore this fascinating field. From my initial training on the basics of cleanroom procedures to being assigned an independent investigation, I have come a long way in my research career. This has been a great first exposure to the field of experimental semiconductor physics and the processing industry. Mr. Yun Zhang (a senior PhD student) served as a mentor and guide, passing on

most of his knowledge and offering suggestions where needed. His day-to-day supervision in the lab, and the endless support extended when compiling results made him an indispensable part of this study. Both Dr. Shen and Yun have been patient with my countless mistakes and have only offered constructive criticism throughout. Dr. Russell Dupuis, by agreeing to be the second reader for this thesis, has helped shape the final outcome of this research and crystallize the results. Through occasional interactions with him, I have learned the importance of discipline and dedication in a research career. I have made countless visits to his lab for measurements, and the staff has been very supportive and encouraging of my endeavor.

The Undergraduate Research Opportunities Program (UROP) is gratefully acknowledged for the award of a grant under the President's Undergraduate Research Award (PURA). The Student Faculty Committee (SFC) award for best undergraduate research poster helped encourage my efforts by recognizing the work done thus far.

7. References

[1] Sze, S. M. (1981). Physics of Semiconductor Devices, John Wiley & Sons.

[2] Zangwill, A. (1988). Physics at Surfaces, Cambridge University Press.

[3] Zeghbroeck, B. V. (2004). Principles of semiconductor devices, Colorado State University.

[4] Pierret, R. (1996) Semiconductor Device Fundamentals. Addison Wesley Longman. Image courtesy Alison Chaiken/GNU Free Documentation License.

[5] Williams, R. (1990). Modern GaAs Processing Methods, Artech House.

[6] H.K. Cho, T. H., J.W. Bae, I. Adesida (2005). "Characterization of Pd/Ni/Au ohmic contacts on p-GaN." Solid-State Electronics **49**: 774–778.

[7] Chen-Fu, C., C. C. Yu, et al. (2000). "Low-resistance ohmic contacts on p-type GaN using Ni/Pd/Au metallization." Applied Physics Letters **77**(21): 3423-5.

[8] Jong Kyu, K., L. Jong-Lam, et al. (1998). "Low resistance Pd/Au ohmic contacts to p-type GaN using surface treatment." Applied Physics Letters **73**(20): 2953-5.

[9] Qiao, D., L. S. Yu, et al. (2000). "A study of the Au/Ni ohmic contact on p-GaN." Journal of Applied Physics **88**(7): 4196-200.

[10] Koide, Y., T. Maeda, et al. (1999). "Effects of annealing in an oxygen ambient on electrical properties of ohmic contacts to p-type GaN." Journal of Electronic Materials **28**(3): 341-346.

[11] Sheu, J. K., Y. K. Su, et al. (1999). "High-transparency Ni/Au ohmic contact to p-type GaN." Applied Physics Letters **74**(16): 2340-2342.

[12] Chen, L.-C., J.-K. Ho, et al. (1999). "Effect of heat treatment on Ni/Au Ohmic contacts to p-type GaN." Physica Status Solidi (A) Applied Research **176**(1): 773-777.

[13] Fan, Z., S. N. Mohammad, et al. (1996). "Very low resistance multilayer ohmic contact to n-GaN." Applied Physics Letters **68**(12): 1672.

[14] Motayed, A., A. V. Davydov, et al. (2002). "High-transparency Ni/Au bilayer contacts to n-type GaN." Journal of Applied Physics **92**(9): 5218-27.

[15] Guo, J. D., C. I. Lin, et al. (1996). "A bilayer Ti/Ag ohmic contact for highly doped n-type GaN films." Applied Physics Letters **68**(2): 235-7.

[16] Yun-Li, L., J. W. Graff, et al. (2001). Novel polarization enhanced ohmic contacts to n-type GaN, Wiley-VCH.

[17] Lin, Y.-J. and C.-T. Lee (2000). "Investigation of surface treatments for nonalloyed ohmic contact formation in Ti/Al contacts to n-type GaN." Applied Physics Letters **77**(24): 3986-3988.

[18] Graff, et al. (2000). "Low-resistance ohmic contacts to p-type GaN." Applied Physics Letters **76**(19): 2728-2731.

[19] Sussman-Fort, S.E., Hantgan, J.C. (1988). "SPICE Implementation of Lossy Transmission Line and Schottky Diode Models" Transactions on Microwave Theory And Techniques **36**(1): 153-155.